International Journal for
Restoration of Buildings
and Monuments
Vol. 9, No 6, 663–682 (2003)

Validation of the Salt Diffusion Coefficient in Porous Materials

A. S. Poupeleer[1], J. Carmeliet[1,2], S. Roels[1] and D. Van Gemert[3]
[1]Laboratory of building physics, Department of civil engineering, K.U.Leuven, Heverlee, Belgium
[2]Department of physical aspects of the building environment, Faculty of civil engineering, T.U.Eindhoven, Nederland
[3]Reyntjens Laboratory of building materials, Department of civil engineering, K.U.Leuven, Heverlee, Belgium

Abstract

The durability of porous building materials largely depends on the transport of liquids and dissolved salts into the material. When the moisture dries out, salts will crystallise introducing important forces in the solid matrix of the porous material. These interaction forces may result in cracking of the material. To study the salt degradation of porous building materials it is necessary to analyse in detail salt transport in (cracked) porous material. In general, salt transport modelling includes different processes: diffusive and convective salt transport, ion adsorption at the pore walls, salt crystallisation and dissolution. In this paper, we analyse in detail the experimental determination of the salt diffusion coefficient of Na_2SO_4 in fully water saturated ceramic brick by using a natural diffusion test. The diffusion coefficient is assumed to depend on the salt concentration. However, it appears that a rotational convective flow gives rise to a three dimensional combined diffusion convection transport.

Keywords: Salt transport, natural diffusion test, salt diffusion coefficient, rotational convective flow, convection.

Bestimmung des Koeffizienten der Salzdiffusion in porösen Werkstoffen

Zusammenfassung

Die Beständigkeit poröser Werkstoffe des Bauwesens hängt weitgehend vom Transport von Flüssigkeiten und darin gelösten Salzen in den Werkstoff hinein ab. Wenn ein Werkstoff wieder austrocknet, kristallisieren Salze im porösen Gefüge aus. Dieser Vorgang kann im Feststoffgerüst bedeutende Kräfte hervor rufen. Die Wechselwirkung mit diesen Kräften kann zur Rissbildung im Werkstoff führen. Um die zerstörende Wirkung von Salzen in porösen Werkstoffen des Bauwesens untersuchen zu können, ist es notwendig, den Salztransport in (gerissenen) Werkstoffen in seinen Einzelheiten zu analysieren. Im allgemeinen werden beim Modellieren des Salztransportes unterschiedliche Prozesse berücksichtigt: diffusiver und konvektiver Salztransport, Ionenadsorption auf den Wänden der Poren, Kristallisieren und Auflösen von Salzen. In diesem Beitrag analysieren wir Ergebnisse von Versuchen zur Bestimmung des Koeffizienten der Salzdiffusion von Na_2SO_4 in vollständig wassergesättigten Proben aus gebranntem Ziegelstein unter Verwendung einer natürlichen Diffusionszelle. Es wird dabei angenommen, dass der Diffusionskoeffizient von der Salzkonzentration abhängt. Es stellt sich jedoch heraus, dass rotierendes konvektives Fließen zu einem dreidimensionalen kombinierten Transport mit diffusiven und konvektiven Anteilen führt.

Stichwörter: *Salztransport, natürlicher Diffusionstest, Koeffizient der Salzdiffusion, rotierendes konvektives Fließen, Konvektion.*

1 Introduction

The durability of porous building materials largely depends on the transport of liquids and dissolved salts into the material [1, 2]. When the moisture dries out, salts will crystallise introducing important forces in the solid matrix of the porous material [3, 4]. These interaction forces may result in cracking of the material. Micro cracks regularly appear in porous building materials due to accidental mechanical overloading, by restrained swelling / shrinking, by repeated hygrothermal loading and by chemical processes. Due to the presence of cracks the penetration of salt solutions accelerates, resulting in a further increase of the damage rate [5, 6]. In this way, the 'damage circle' becomes closed [7] (Fig. 1). A second salt damage process is related to the salt hydratation [8, 9] accompanied with volume expansion. When the expansion is restrained, important interaction forces may lead to damaging of the material.

Hence, to study the salt degradation of porous building materials it is necessary to analyse in detail salt transport in (cracked) porous material. In general, salt transport modelling includes different processes: diffusive and convective salt transport, ion adsorption at the pore walls, salt crystallisation and dissolution. In this paper, we analyse in detail the experimental determination of the salt diffusion coefficient in saturated ceramic brick. Especially, we investigate the influence of possible convective processes due to salt density differences.

In literature several methods to determine the salt diffusion coefficient are proposed. Since chloride ingress is one of the main causes of rebar corrosion in reinforced concrete, a lot of research focused on the determination of chloride diffusion coefficient. Due to the low diffusion coefficient of concrete, traditional diffusion tests are very time-consuming. Whiting [10] introduced the 'Rapid Chloride Permeability Test', also called migration test, where the diffusion process is accelerated by an electric field. The method was adapted by Andrade [11] introducing effective or apparent diffusion coefficients. An apparent diffusion coefficient describes both the salt flow as well as the chemical reactions between the salt ions and the cement paste. Marchand [12] modelled migration test results, including ion diffusion with electric field by solving the extended Nernst-Planck/ Poisson set of equations and including chemical reactions between ions and cement paste. A good agreement between test results and simulations was obtained. However, it is noted that the amount of chloride ions in a migration test is relatively small compared to the amount of ions in a natural diffusion test [13]. As a result, processes such as ion adsorption are underestimated. It is questioned whether a migration test covers the same transport mechanisms as in natural diffusion tests.

Natural diffusion in concrete is commonly analysed determining concentration profiles of water-soluble chlorides measured in real concrete structures exposed to marine environment or to de-icing salts [14, 15, 16]. The measured profiles are

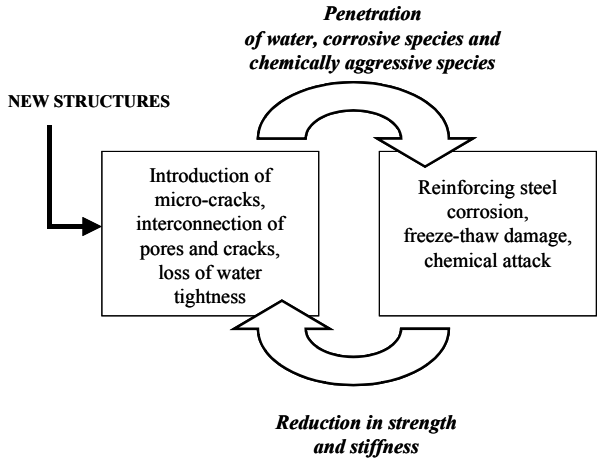

Figure 1: Cyclic degradation process (following Mehta [1]).

compared with numerical solutions of Fick's second law only describing diffusion in water saturated porous media. The obtained diffusion coefficients are described by parametric functions taking into account the cement type, the W/C-factor of the concrete and the exposure period in time [14, 17]. Drawback of the method is that the different processes influencing chloride diffusion, such as ion adsorption, possible blocking by crystallized salts (unsaturated conditions) and chemical reactions are joined into an apparent diffusion coefficient. Moreover, full water saturation is generally assumed, which does not agree with the real exposure conditions.

To more accurately account for ion adsorption, Coussy used a coupled diffusion-sorption equation [18]. The adsorption process is described by a sorption isotherm, experimentally determined by Francy [19].

Buchwald [20] measured the diffusion coefficient as function of the degree of water saturation using the impedance spectroscopy technique for different materials. They showed the diffusion coefficient to decrease non-linearly with degree of saturation.

Kuhl [21] investigated the dependence of the diffusion coefficient on salt concentration. He compared the thermodynamical model with the diffusion model based on the theory of the ionic clouds [22] considering ion-ion interactions by the electrostatic coupling [23]. The theory of the ionic clouds describes the interaction of electrically charged particles by electrostatic forces and viscous forces. This so-called 'Nernst treatment' leads to an expression for the dependence of the diffusion coefficient on the concentration of infinite dilute solutions. For higher concentrations the mean free distance between migration ions becomes smaller and conse-

quently repelling and attracting electrostatic forces connect the Brownian movements of the ions. The result of these forces is a reduction of the macroscopic ionic drift, also called the relaxation effect ('Nernst-Hartley treatment'). According to this theory the diffusion coefficient is written as a function of the mean molar activity and the molar concentration [24]. Next to the ion-ion interactions also the solvent plays an interfering role. It forms the boundary layer around the moving ions. They interact due to the flow field with the solvent and with the ions in their environment. This phenomenon proposed by the 'Onsager-Fouss treatment' is the electrophoretic effect, which results in an extra correction factor for the diffusion coefficient. This study shows that the molecular diffusion coefficient is not a constant, but function of the concentration due to the influence of electrostatic ion-ion interactions and ion-solvent interactions. In literature measurements of the free molecular diffusion coefficients for different salts in function of the concentration are available [25, 26].

From this literature overview, we learn that the experimental determination of the diffusion coefficient remains complex. The diffusion coefficient is dependent on salt concentration, degree of water saturation and it is difficult to distinguish between concurrent processes such as diffusion, convection, ion adsorption and chemical reactions.

The aim of this paper is to characterise accurately the diffusive transport of Na_2SO_4 in fully water saturated conditions excluding ion adsorption, chemical reactions and crystallisation. In this study ceramic brick was used, which shows no ion adsorption, is chemically inert and has a sufficient high diffusion coefficient limiting the measurement time (an exterior electric field is not needed). Dependence of the diffusion coefficient on concentration is taken into account. However, it will be shown that although pure diffusion was envisaged, convective flow occurred due to salt density differences complicating the determination of the diffusion coefficient.

2 Testing Procedure and Measurement Data

The test set-up to measure the transport process of a single electrolytic salt Na_2SO_4 in a saturated brick is schematically represented in figure 2.

The experimental diffusion cell consists of two vessels containing different salt concentrations with in between a water saturated brick sample (Fig. 2). The volumes of the vessels are approximately 0.0013 m³, the diameter is 0.1031 m, the length is 0.16 m and on top there are three tubes with diameter 0.017 m. The vessels are filled up to 0.1266 m height. Vessel A contains a high concentration of Na_2SO_4 (0.5 or 1.0 M) whereas vessel B contains distillated water. The specimens are circular discs sealed at the lateral sides by epoxy. Four brick specimen are tested. The three tubes on top of the vessels are provided for measuring the concentration with a conducti-

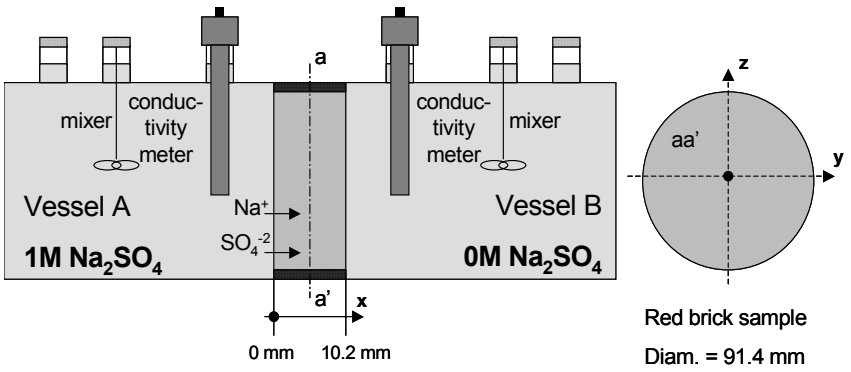

Figure 2: Schematical representation of the diffusion cell test set-up of sample 'a'

vity meter, for stirring up the liquid to level out possible concentration gradients and to prevent overflow. To prevent evaporation the tubes that are not in use are closed with a rubber cap. However, it is impossible to prevent a slight evaporation during the long execution time of the test. The whole set-up is kept in isothermal conditions (21°C).

The concentration of each vessel is measured placing a conductivity meter into the vessel at discrete time steps. The conductivity is a cumulative measure for ionic concentration of a solution. The conductivity meters are calibrated measuring the conductivity at different known concentrations.

The boundary conditions of the test are not constant due to the limited volumes of the vessels. Under the concentration gradient the concentration in vessel A is decreasing, while the concentration in vessel B increases. Consequently, the concentration gradient varies with time.

The test results for the four bricks are shown in figure 3. The specimens differ in thickness, diameter and initial concentration difference. As expected the concentration in vessel B increases more rapidly with decreasing thickness (d), increasing diameter (D) and concentration difference (ΔC).

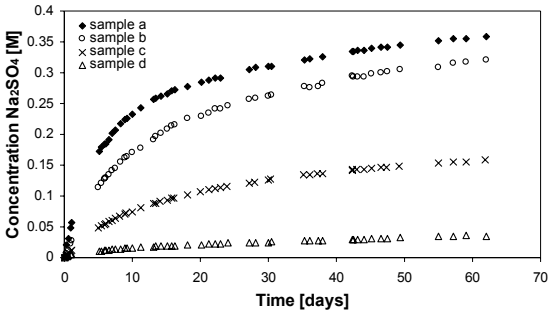

	D [mm]	d [mm]	ΔC [mol/l]
sample a	91.4	10.2	1.0
sample b	91.0	17.0	1.0
sample c	91.4	9.5	0.5
sample d	25.7	10.2	1.0

Figure 3: Concentration in function of time for the tested bricks a, b, c and d in vessel B.

3 Simulations

3.1 Global Transport

The general coupled liquid water and salt diffusion-convection transport including an external electric field can be formulated by the equations:

WATER

One dimensional isothermal water transport:

$$C(p_c)\frac{\partial p_c}{\partial t} = \frac{\partial}{\partial x}\left(K(p_c)\frac{\partial p_c}{\partial x} \right) \tag{1}$$

SALT

Flux density of each dissolved species:

$$q_i = -z_i u_i F c_i \nabla\Phi - \frac{\phi D_i(c_i)}{\tau}\nabla c_i + c_i v \tag{2}$$

Material balance:

$$\frac{\partial c_i}{\partial t} = -\nabla q_i \tag{3}$$

Electro neutrality condition:

$$\sum_i z_i c_i = 0 \tag{4}$$

where p_c is the capillary pressure, $C(p_c)$ is the moisture capacity, $K(p_c)$ the moisture permeability, z_i is the number of proton charges by an ion, u_i is the mobility, F is the

Faraday constant, Φ is the potential, $D_i(c_i)$ the molecular diffusion coefficient in free solution in function of the concentration, ϕ the porosity, τ the tortuosity, ∇c_i the concentration gradient, v the bulk velocity.

These equations for the salt transport are only correct for dilute solutions. The average velocity v of the salt solution for example does not correspond to the solvent velocity in concentrated solutions. Only for dilute solutions the approximation is accurate. Secondly, the transport properties are taking into account friction forces of a solute species with the solvent, but interactions with other solutes are neglected. Thirdly, the driving force for diffusion should be an activity gradient instead of a concentration gradient. Only in extremely dilute solutions these two correspond. The correct driving force for diffusion and migration would be the electrochemical potential gradient $\nabla \mu_i$ including both transport phenomena. To determine the convective velocity v also the liquid water transport equations are required. Despite the mentioned limitations, we will assume the equations to be valid.

Applying the set of equations to the present test set-up of the diffusion cells the three dimensional transport processes for Na_2SO_4 can be approximately described by the diffusion-convection equation:

$$\phi \frac{\partial C_s}{\partial t} = \nabla \frac{\phi D}{\tau} \nabla C_s + \phi \dot{u} \nabla C_s \tag{5}$$

where C_s is the salt concentration and $\dot{u}$ is the pore velocity. Note that the term describing salt transport due to an external electric field is omitted. This equation has to be solved taking into account the geometry of the sample and the test set-up, the initial and boundary conditions. The boundary conditions (i.e. the concentration in the vessels) change with time and can be determined by solving the salt balance in the different vessels. The salt balance states that the change of concentration in the vessels is a result of the salt flux going out or into the vessel.

Possible liquid transport in saturated conditions is described by Darcy's law. Boundary conditions for liquid transport are the pressure heads in the vessel. Radial fluxes of liquid and salt through the outer surface of the sample are set equal to zero.

3.2 Pure Diffusion

Diffusion is the transport due to a concentration gradient. The diffusion coefficient D' is given by [20]:

$$D'(C_s) = \frac{D(C_s)\phi}{\tau} \tag{6}$$

with $D(C_s)$ the molecular diffusion coefficient of the salt in function of its concentration, ϕ the total open porosity (because the sample is totally saturated) and τ the tortuosity. The molecular diffusion coefficient at low concentration (dilute solution) can be theoretically calculated as the weighted average of the ion diffusion coefficients of Na^+ and SO_4^{2-} (D (0 M) = 1.23e-9 m²/s). For the molecular diffusion coefficient at higher concentrations the values experimentally defined by Robinson [26] (Fig. 4) are taken. The tortuosity is estimated based on measured vapour resistance factors varying between 10.36 and 14.34 [27]. Using the measured porosity (ϕ = 23 %), the tortuosity can be estimated ranging between 2.4 and 3.3. An averaged value of 3 is taken. This leads for example to a diffusion coefficient of 9 e-11 m²/s at low concentration.

With this reasonable estimate of the concentration dependent diffusion coefficient D'(C_S) the different tests are calculated and compared to the test results (figure 5). In all cases it is obvious that diffusive transport (black lines in figure 5) is not fast enough to predict the measured data. Even in the extreme situation (dotted lines in figure 5) with a porosity of 100 % and a tortuosity of 1, which corresponds to diffusion in a free solution, the simulation does not agree. The curves are not steep enough in the beginning of the process, but too steep near the end. The explanation should be searched in the fact that another physical transport phenomenon is taking place.

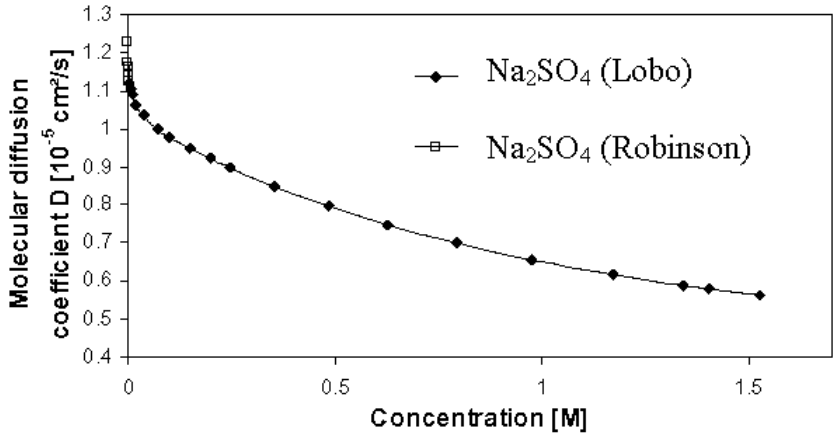

Figure 4: Molecular diffusion coefficient of Na_2SO_4 in function of the concentration. [25, 26]

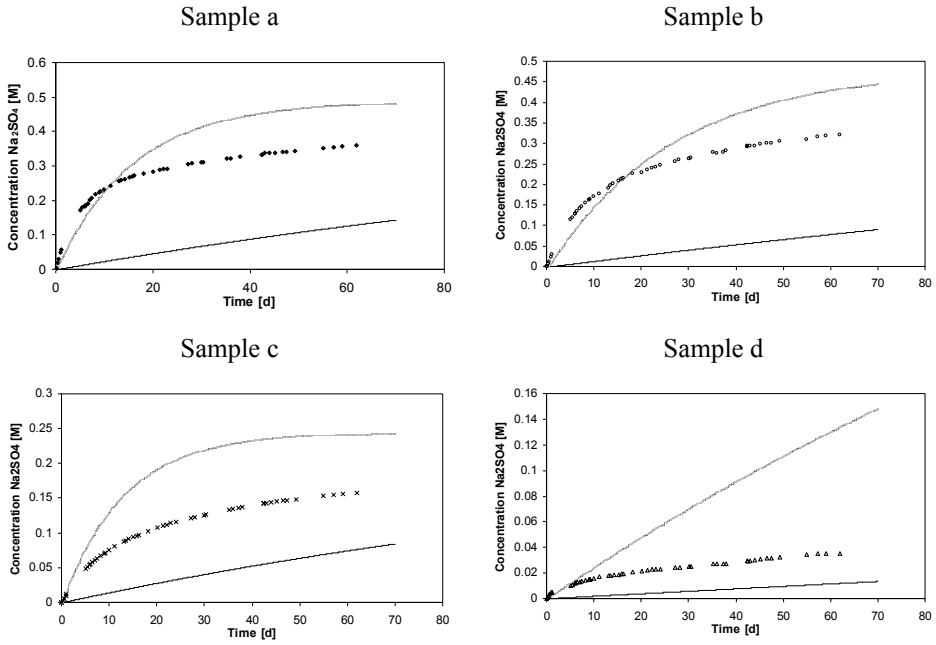

Figure 5: Simulations with pure diffusion in the bricks and assuming transport in free solution
◆ measured data; ━━ diffusion in brick; —— diffusion in free solution

3.3 Convection

Convective transport in the diffusion cells with equal pressure head (height of liquid) at both sides is not expected. However, the hydrostatic pressure profile over the height of the sample will be different in both vessels as a result of the density difference between the two solutions at different concentration. Figure 6 gives the change of density in function of the concentration between 0 and 1 M (limits in the tests). The pressure difference is:

$$\Delta P = P_A - P_B = \rho(C_{s,A})gz - \rho(C_{s,B})gz \qquad (7)$$

where P is the pressure, ρ the density, g the gravity and z the depth. The pressure difference is the driving force for a convective transport mechanism. The time evolution of the pressure difference profile is given in Fig. 7.

At the beginning (Fig. 7,I) the pressure difference is positive leading to a convective flow from vessel A (high concentration) to vessel B (low concentration). The pressure difference is lower at the top than at the bottom of the specimen resulting in a convective flow decreasing with height. According to the mass balance principle,

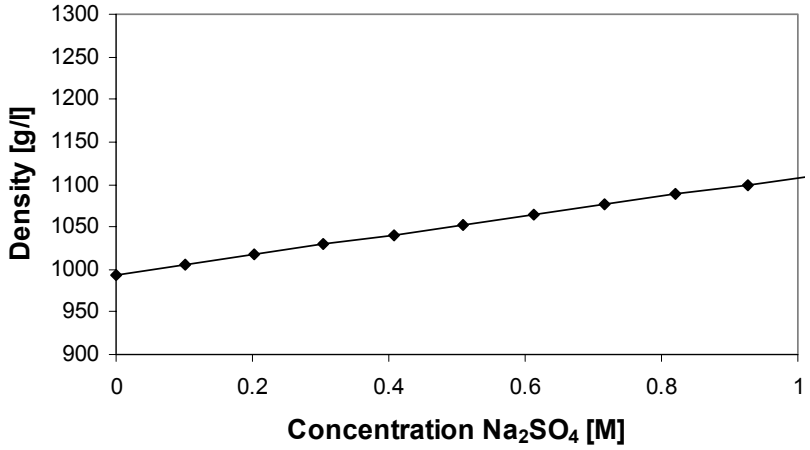

Figure 6: Density of Na_2SO_4 in function of the concentration [24]

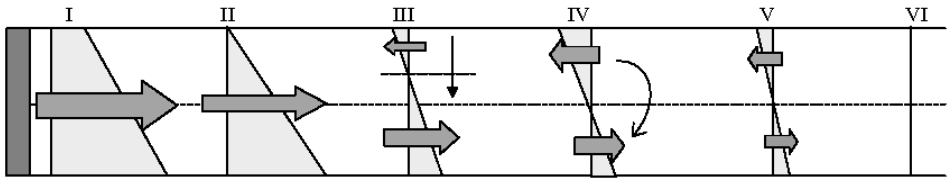

Figure 7: Pressure difference profiles over the sample in function of time

the heights of the liquids in the vessels change, which results in a change of the pressure in the vessels. The pressure in vessel B increases while the pressure in vessel A decreases. This results in a drop of the pressure difference with evolving time (Fig. 7, II). After a certain period of time, the pressure difference in the upper part of the specimen becomes negative and a backwards convective flow appears (Fig. 7, III). The height of the liquid in vessel B remains increasing until pressure equilibrium is reached (Fig. 7, IV): i.e. the pressure difference at top and bottom becomes equal. This also means that a fully developed rotational convective flow appears: forward and backward convective fluxes are equal but in opposite direction. The development of the rotational convective flow takes half an hour to several hours depending on the geometry of the test-up. From then on the rotational convective flow pattern remains, but gradually lowers with time as the concentrations at both sides approach each other (Fig. 7, V). This second stage of the process takes several months.

For the simulation of the convective transport the value of the water permeability *K* has to be known. The liquid water permeability is determined form air permeability measurements and ranges from 1.0e-7 to 2.5e-7s [28]. Additionally liquid water permeabilities are measured using a pressure head difference over the sample giving a value of K = 0.7e-7s.

3.4 Combined Diffusion-Convection Process

As described above, the real transport process is a combination of diffusion and convection (Fig. 8). First one dimensional diffusion occurs as expected from vessel A to B. Secondly, a rotational convective flow due to the density differences in the vessels appears. Due to this rotational convective flow characteristic concentration profiles develop. At the bottom the concentration in sample is at high level due to dominant forward convective flow, while at the top the backward flow results in low concentration profiles. Consequently, diffusive fluxes occur also in the vertical direction of the sample. Therefore, a three-dimensional approach is necessary to capture all occurring diffusive and convective flows. The transport equations are solved using an implicit control volume (CV) method.

The results of the calculations are given for the four different situations in figure 9. In all the cases it is obvious that only diffusion can not predict the measured data (Fig. 5). Diffusion-convection results are in much better accordance. Figure 9a

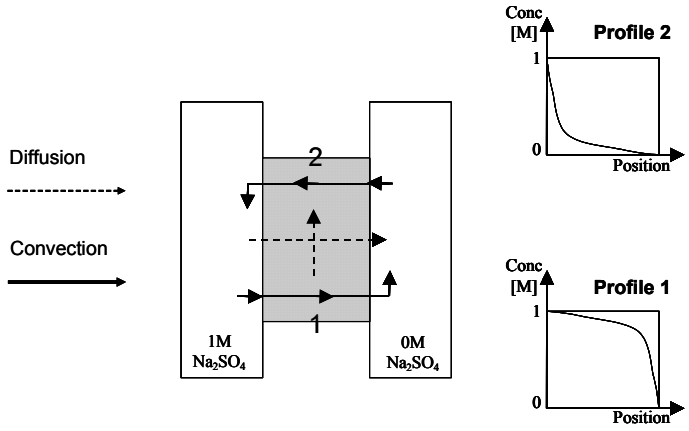

Figure 8: Combined diffusion-convection transport process

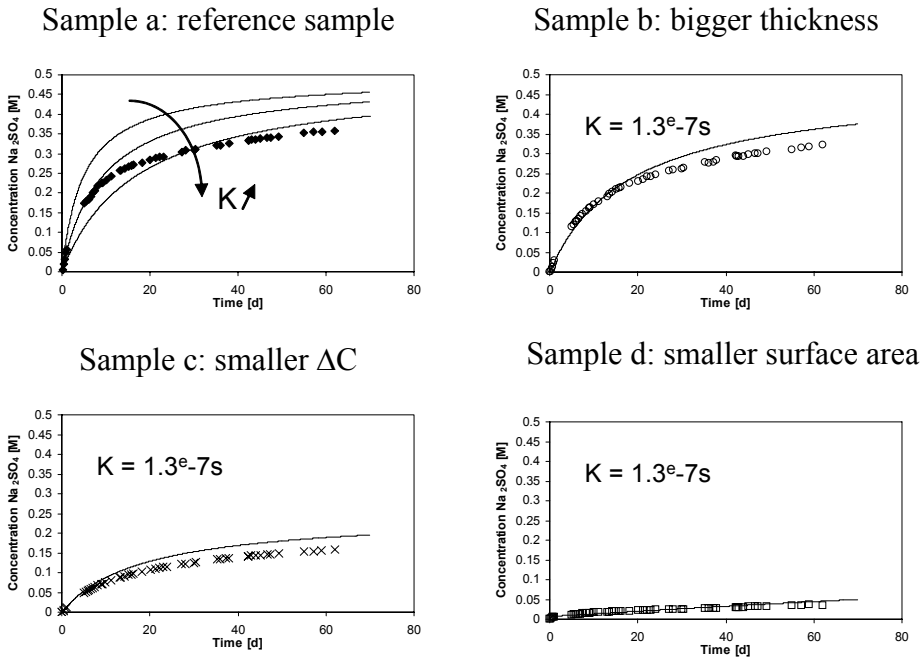

Figure 9: Simulation results of the combined diffusion-convection transport process

gives simulations for the set of measured liquid water permeabilities (0.7e-7s, 1.3e-7s and 2.5e-7s). The results show a high sensitivity to the liquid water permeability. The measurement data fall into the set of calculated curves for the first 30 days. Hereafter, the agreement decreases, which may be explained by the inhomogeneity of the brick: rotational convective flow can be highly influenced by changes of the liquid water permeability with height. Also measurement inaccuracy during the long measuring time caused by evaporation, changing of water heights in the vessels due to the placement of conductivity meters or stirring discontinuity can influence the results.

The calculated forward and backward volume fluxes (Fig. 10) in function of time for the reference sample ‘a’ show that the initial flux is going from vessel A to vessel B. After 13 minutes a small backward flow starts to flow gradually becoming equal to the forward flow. In the inset of figure 10, we observe that the convective fluxes gradually become smaller until they finally approach zero when the concentration in the both vessels is equal.

Figure 11 shows the change of the concentration distribution in the sample. Pure diffusion moves a uniform concentration front slowly into the material. After 500 hours the concentration front has just reached the other side of the specimen. In the

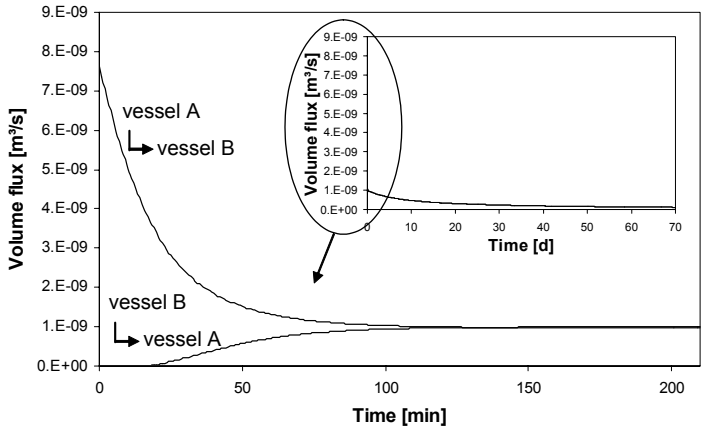

Figure 10: Simulation results of the combined diffusion-convection transport process

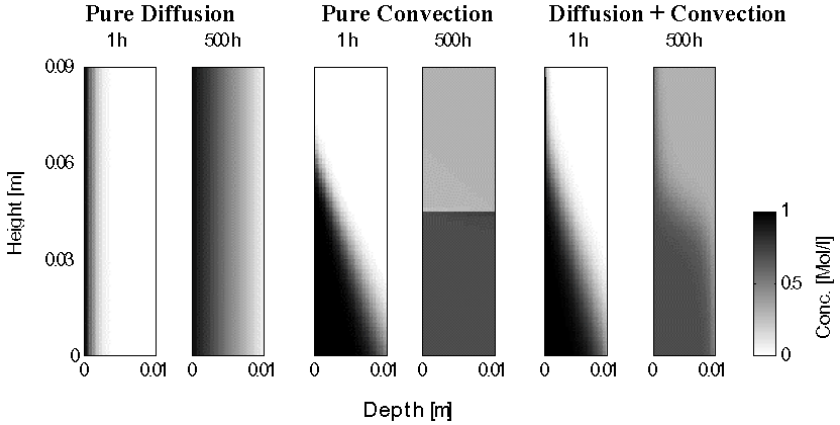

Figure 11: Simulation results of the combined diffusion-convection transport process

case of pure convection, we observe that break-trough of the concentration front has already occurred within the first hour. After 500 hours the fully developed rotational flow results in two distinct zones with constant concentration. Finally, the results of the diffusion-convection process are shown.

Detailed profiles at the top and at the bottom of the sample for the pressure head and concentration in function of the thickness are given in figure 12. As expected the slope of the pressure lines changes sign during the first hour indicating an evolution

from forward to backward convective flow. As a result the ingress of the concentration front remains limited and even returns slowly towards the original situation. At the bottom of the sample the pressure difference over the sample is high at the beginning of the test and drops in function of time. The direction of the convective flow remains forward and the slope of the pressure lines remain positive. Due to forward convective flow the concentration front penetrates continuously deeper into the material.

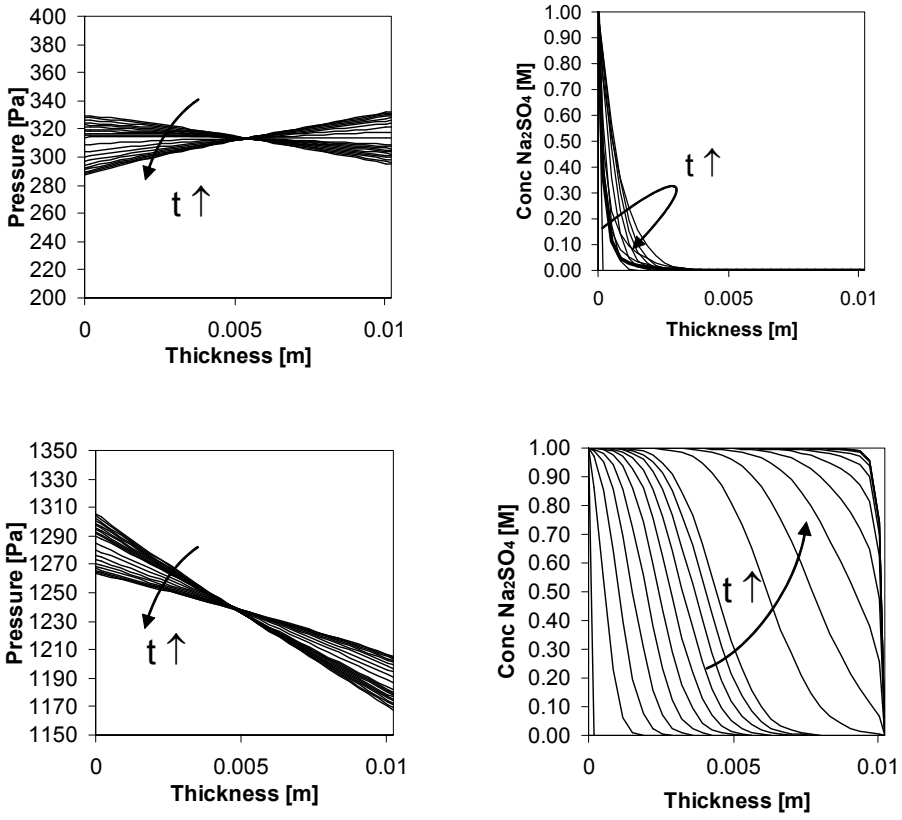

Figure 12: Pressure and concentration profiles of the reference sample during the first hour at the top (upper figures) and the bottom (lower figures) of the sample.

4 Conclusions

In this paper the diffusive transport of Na_2SO_4 in fully water saturated ceramic brick is analysed using a natural diffusion test. The diffusion coefficient is assumed to depend on the salt concentration. Complex processes such as ion adsorption, chemical reactions and crystallisation are excluded from the study. It is found that a concentration dependent diffusion coefficient can not reproduce the measurement data.

Due to the concentration differences the density of the liquid at both sides of the sample differs resulting in a hydrostatic pressure difference. The pressure difference is the driving force for a convective transport mechanism. At the beginning the pressure difference is positive leading to an important forward convective flow and a fast break-trough of the concentration front. After a certain period of time, a rotational convective flow develops: forward convective flow at the bottom and backward convective fluxes at the top of the specimen. The rotational convective flow gives rise to a three dimensional combined diffusion convection transport. Simulations taking into account this transport process showed good agreement with the measured data. Since convection was found to be the dominant driving force, it is concluded that the test set-up is less suited for an accurate determination of the diffusion coefficient.

The convective mechanism depends on the height of the specimen, the ratio between liquid water permeability and diffusion coefficient, the dependence of the density on salt concentration. The test for a given salt and material can only be improved by reducing the height of the specimen. An alternative is the determination of the diffusion coefficient by tracer experiments [29].

References

1. Sandberg P., ‘Systematic collection of field data for service life prediction of concrete structures’, Durability of concrete in saline environment, pp. 7-22; (1996)
2. Lars-Olof Nilsson, ‘Moisture in marine concrete structures –studies in the BMB-project 1992-1996’, Durability of concrete in saline environment, pp. 23-47; (1996)
3. Evans I.S., ‘Salt crystallizations and rock weathering: a review’, Revue de Géomorphologie Dynamique (19), pp. 153-177; (1970)
4. Winkler E.M., Singer P.C., ‘Crystallization pressure of salts in stone and concrete’, Geol Soc Am Bull 83 (11): pp. 3509-3514; (1972)
5. Winkler E.M., ‘Weathering agents’, Stone in Architecture, Chapter 5, pp. 111-141; (1994)

6. Biczók I., 'Concrete corrosion and concrete protection', ed. Akademiai Kiado Budapest; (1964)
7. Mehta P.K., 'Concrete technology at the crossroads – problems and opportunities', Proceedings P.K. Mehta Symp. on Durability of Concrete, Nice, May 21, pp. A1-A33; (1994)
8. Mortensen H., 'Die Salzsprengung und ihre Bedeutung für die regional klimatische Gliederung der Wüsten', Petermann's Geogr Mitt, pp. 133-135; (1933)
9. Winkler E.M., Wilhelm E.J., 'Saltburst by hydratation pressures in architectural stone in urban atmosphere', Geol Soc Am Bull 81(2):567-572; (1970)
10. Whiting D., 'Rapid measurement of the chloride permeability of concrete', Public Roads, V. 45 (3), pp. 101-112; (1981)
11. Andrade C., Alonso C. and Acha M., 'Chloride diffusion coefficient of concrete containing fly ash calculated from migration tests', Corrosion and corrosion protection of steel in concrete, Vol.2, pp. 783-793; (1994)
12. Marchand J., 'Modeling the behavior of unsaturated cement systems exposed to aggressive chemical environments', Materials and structures, Vol. 34, May 2001, pp. 195-200; (2001)
13. Page C.L., Short N.R. and El Taras A., 'Diffusion of chloride ions in hardened cement pastes', Cement and concrete research, Vol. 11, pp. 395-406; (1981)
14. Lim C.T.E., Ong K.C.G., Law K.H. and Paramasivam P., 'Concentration profiles of water-soluble chloride in 32 year-old marine concrete piles', Proceedings of the 5th CANMET/ACI International conference on recent advances in concrete technology, Singapore, July 29-August 1, editor : Malhotra V.M., volume SP-200, pp.51-64; (2001)
15. Schueremans L. and Van Gemert D., **'**Service life prediction of reinforced concrete structures, based on in-service chloride penetration profiles', 8DBMC, 8th International Conference on Durability of Building Materials and Components, May 30 - June 3, Vancouver, Canada, pp. 83- 93; (1999)
16. Polder R.B., Hug A., 'Penetration of chloride from de-icing salt into concrete from a 30 year old bridge', TNO Building and Construction Research, Rijswijk, The Netherlands, Heron, vol. 45 (2), pp. 109-124; (2000)
17. Takewaka K., Mastumoto S., 'Quality and cover thickness of concrete based on the estimation of chloride penetration in marine environments', American concrete institute special publication, (ACI SP-109), ed. by V.M. Malhotra, Proc. Second Int. Conf. on Concrete in marine Environment, ST. Andrews-by-the-Sea, New Brunswick, Canada, pp. 381-400; (1980)
18. Coussy O., Ulm F.-J., Mainguy M., 'A short-course on environmental mechanics of concrete', lecture notes

19. Francy O., 'Modélisation de la penetration des ions chlorues dans les mortiers partiellement saturés en eau', INSA de Toulouse, PhD Thesis; (1998)
20. Buchwald A., 'Determination of the ion diffusion coefficient in moisture and salt loaded masonry materials by impedance spectroscopy', 3rd Int. PhD Symposium 11.-13.10.2000, Vienna; Vol 2, pp. 475-482; (2000)
21. Kuhl D., Meschke G., 'Computational modeling of transport mechanisms in reactive porous media – application to calcium leaching of concrete', Computational modeling of concrete structures, eds. Bicanic et al., pp. 476-482; (2003)
22. Debey P., Hückel E., 'Zur Theorie der Elektrolyte.I. Gefrierpunktserniedrigung und verwandte Erscheinungen', *Physikalische Zeitschrift* 24 (9), 185-206; (1923)
Debey P., Hückel E., 'Zur Theorie der Elektrolyte.II. Grenzgesetz für die elektrische Leitfähigkeit', *Physikalische Zeitschrift* 24 (15), 305-325; (1923)
Debey P., Hückel E., 'Report on conductivity of strong electrolytes in dilute solutions', in: C. Desche (Ed.), The theory of strong electrolytes. A general discussion, Vol. 23, Transactions of the Faraday Society, 334-340; (1927)
23. Nernst W., 'Zur Kinetik der in Lösung befindlichen Körper. I. Theorie der diffusion', Zeitschrift für physikalische Chemie 2, 613-637; (1888)
24. Hartley G., 'Theory of the velocity of diffusion of strong electrolytes in dilute solution', *The London, Edinbourgh and Dublin Philosophical Magazine, and Journal of Science* 12 (77), 473-488; (1931)
25. Lobo V., 'Handbook of electrolyte solutions'. Part A, Elsevier, Amsterdam; (1989)
26. Robinson R.A., Stokes R.H., 'Electrolyte solutions', Second editions, London Butterworths; (1970)
27. Roels S., Carmeliet J., Hens H., Hamstad project WP1: Final report: 'Moisture transfer properties and materials characterization', February, KULeuven, Belgium, Hamstad-document, KUL2003-18; (2003)
28. Carmeliet J., Descamps F., Houvenaghel G., 'A multiscale network model for simulating moisture transfer properties of porous media', Transport in porous media 35: 67-88; (1999)
29. Plagge R., Grunewald J., 'Determination of solute transport from laboratory tracer experiments', Building Physics 6th Nordic Symposium, pp. 531-538; (2002)

Anne-Séverine Poupeleer, ir. studied civil engineering at the K.U.Leuven, Belgium. From 2000 till 2001 research associate at the Group of Building Materials, Civil Engineering, K.U.Leuven. From 2001 till 2003 research associate at the Laboratory of Building Physics, K.U.Leuven, Belgium, working at a PhD on 'Transport of water and dissolved salt in cracked porous materials'.
Anne-Severine.Poupeleer@bwk.kuleuven.ac.be

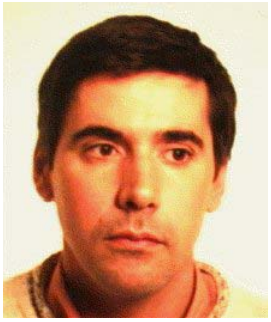

Jan Carmeliet, dr. ir. earned his Ph.D. at the Katholieke Universiteit Leuven, 1992 with highest distinction, on 'Durability of fibre-reinforced renderings for outside insulation: a probabilistic approach based on the non-local continuum damage mechanics'. He is an associated professor teaching Building Engineering, Building Physics and Project Engineering. Since 2001, he is also a professor at the Technical University of Eindhoven, The Netherlands. His research issues are: heat and mass transfer in heterogeneous, cracked, porous building materials; driving rain; durability physics and mechanics; X-ray computer tomography for moisture transfer identification and non-destructive testing of materials.
jan.carmeliet@bwk.kuleuven.ac.be

Staf Roel, dr. ir. studied engineering-architecture at the K.U.Leuven, Belgium. From 1990 till 1991 research associate at the Group of Building Materials, Civil Engineering, K.U.Leuven. From 1991 till 1995 architectural practice. Since 1995 research associate at the Laboratory of Building Physics, K.U.Leuven, Belgium. In 2000 PhD on 'modelling unsaturated moisture transport in heterogeneous limestone'. Since 2001 part-time assistant professor.
staf.roels@bwk.kuleuven.ac.be

Dionys Van Gemert, dr. ir., is professor of building materials science and renovation of constructions at the Department of Civil Engineering of KULeuven, Belgium. He is head of the Reyntjens Laboratory for Materials Testing. His research concerns repairing and strengthening of constructions, deterioration and protection of building materials, concrete polymer composites.
Dionys.VanGemert@bwk.kuleuven.ac.be

Received November 26th 2003